RSC Advances

PAPER

View Article Online
View Journal | View Issue

Cite this: *RSC Adv.*, 2023, **13**, 15165

Adsorption characteristics of dichloromethane-ethyl acetate/toluene vapor on a hypercrosslinked polystyrene adsorbent†

Yanbing Cao,[ab] Xiaoqi Fei,[acd] Xuanhao Wu,[ab] Haiqiang Wang *[ab] and Zhongbiao Wu[ab]

Dichloromethane (DCM), a typical representative of chlorinated volatile organic compounds (CVOCs), is usually exhausted along with other volatile organic compounds (VOCs), such as toluene and ethyl acetate, in industrial factories. To address the complexity of the components, the large variation in concentration of each component and the water content of the exhaust gases emitted from the pharmaceutical and chemical industries, the adsorption characteristics of DCM, toluene (MB), and ethyl acetate (EAC) vapors on hypercrosslinked polymeric resins (NDA-88) were studied by dynamic adsorption experiments. Furthermore, the adsorption characteristics of NDA-88 for binary vapor systems of DCM-MB and DCM-EAC at different concentration ratios and the nature of the interaction force with the three VOCs were explored. NDA-88 was found to be suitable for treating binary vapor systems of DCM mixed with low concentrations of MB/EAC, and a small quantity of adsorbed MB or EAC would promote the adsorption of DCM by NDA-88, which is attributed to the microporous filling phenomenon. Finally, the influence of humidity on the adsorption performance of binary vapor systems for NDA-88 and the regeneration adsorption performance of NDA-88 were investigated. The presence of water steam shortened the penetration times of DCM, EAC, and MB, regardless of whether it was in the DCM-EAC or DCM-MB two-component systems. This study has identified a commercially available hypercrosslinked polymeric resin NDA-88, which has excellent adsorption performance and regeneration capacity for both single-component DCM gas and a binary mixture of DCM-low-concentration MB/EAC, providing experimental guidance for the treatment of emissions from pharmaceutical and chemical industries by adsorption.

Received 17th March 2023
Accepted 2nd May 2023

DOI: 10.1039/d3ra01754k

rsc.li/rsc-advances

1 Introduction

Atmospheric environmental safety directly affects the quality of the environment and human health. Volatile organic compounds (VOCs) are one of the main causes of compound pollution and haze in urban agglomerations.[1,2] Chlorinated volatile organic compounds (CVOCs) are often highly toxic and can even be teratogenic, carcinogenic, and mutagenic.[3] Dichloromethane (DCM) is a typical representative CVOCs and one of the widely used organic solvents in the pharmaceutical and chemical industries owing to its high solubility;[4] however, its highly emissive nature makes it difficult to treat DCM.[5] Furthermore, exhaust gas contains not only a large amount of DCM but is also commonly accompanied by some other VOCs, such as toluene (MB) and ethyl acetate (EAC), which are toxic to some extent.[6] Therefore, there is an urgent need to develop efficient, environmentally friendly, and economical DCM treatment technologies for gases mixed with DCM and other VOC compounds.[7]

Adsorption is a traditional processing technology that can effectively treat VOCs at a low cost. Activated carbon is a traditional absorbent used for the removal of VOCs from gas streams with subsequent VOC recovery or other treatments.[8] However, the adsorption process using activated carbon encounters pore blocking,[9] the inefficient desorption of high-boiling solvents,[10] combustion, and hygroscopicity.[11] Thus, researchers have focused on finding superior candidates for the removal and recovery of VOCs from polluted air streams.

Porous resins have also been widely used in the adsorption of various VOCs owing to their controlled pore structure, stable physicochemical properties, and *in situ* regeneration, making

[a]*Key Laboratory of Environment Remediation and Ecological Health, Ministry of Education, College of Environmental Resources Science, Zhejiang University, Hangzhou 310058, P. R. China. E-mail: haiqiangwang@zju.edu.cn*

[b]*Zhejiang Tianlan Environmental Protection Technology Co., Ltd., Zhejiang Provincial Engineering Research Center of Industrial Boiler Furnace Flue Gas Pollution Control, Hangzhou 310058, P. R. China*

[c]*Zhejiang Academy of Special Equipment Science, Hangzhou 310020, P. R. China*

[d]*Key Laboratory of Special Equipment Safety Testing Technology of Zhejiang Province, Hangzhou 310020, P. R. China*

† Electronic supplementary information (ESI) available. See DOI: https://doi.org/10.1039/d3ra01754k

them a preferable substitute for activated carbon in the adsorption treatment of VOCs.[12] Moreover, hypercrosslinked polymeric resin, a kind of porous resin, is a novel adsorbent that has been studied for its good adsorption performance on CVOCs.[13–15] Lu *et al.*[13] found that the adsorption capacity of V-503 resin for toluene with moisture content below 30% was comparable to that of dry resin with high humidity, and the adsorption performance remained high after four adsorption and desorption cycles, with a resolution of up to 95%. Besides, Wang *et al.*[16] prepared a superhydrophobic hypercrosslinked polymeric resin with both microporous and mesoporous structures, which has a higher adsorption capacity for benzene than commercial activated carbon in a humid environment and considerably higher selectivity. These studies have shown that hypercrosslinked polymeric resins are promising adsorbents for removing and recovering CVOCs from polluted vapor streams. However, toxic gases emitted from pharmaceutical and chemical fields not only contain a large number of CVOCs but are also usually mixed with some common VOCs, such as MB and EAC. Current adsorption studies related to hypercrosslinked polymeric resins have mainly focused on single components. There are few studies on two-component adsorption and the interaction between different adsorbates is still unclear.

In this study, DCM was used as the main probe molecule, and a hypercrosslinked polymeric resin (NDA-88) was used as an adsorbent to evaluate its single-component adsorption penetration characteristics. On this basis, the adsorption selectivity of the hypercrosslinked polymeric resin for two-component adsorption of DCM and EAC/MB at different concentration ratios was investigated. Finally, the influence of humidity on the adsorption performance of binary vapor systems on NDA-88 and the regeneration adsorption performance of NDA-88 were investigated. Hopefully, the work reported here can provide new insights into improving the industrial application of hypercrosslinked polymeric resins for the treatment of CVOCs.

2 Experimental

2.1 Materials and characterization

Commercial available hypercrosslinked polymeric resins (NDA-88) with poly(styrene-divinylbenzene) matrix were adopted in this study. The NDA-88 was purchased from Zhengzhou He Cheng New Material Technology Co., Ltd. (Henan, China). The pore texture of the polymeric adsorbents was determined by N_2 isotherm data at 77 K using an adsorption analyzer 3Flex 5.02 (Micromeritics Instrument Co., USA). The thermal stability experiments of NDA-88 were carried out using the TG 209 F3 thermogravimetric analyser (NETZSCH-Gerätebau GmbH) for programmed temperature rise measurements, and the TG and DTG curves obtained are shown in Fig. 1. It can be seen that NDA-88 maintains a stable physical structure up to 400 °C.

Before use, NDA-88 was dried in a vacuum oven at 383 K for 12 h. The dichloromethane, ethyl acetate, and toluene used in the experiments were purchased from Nanjing Specialty Gases Co., Ltd. (Jiangsu, China).

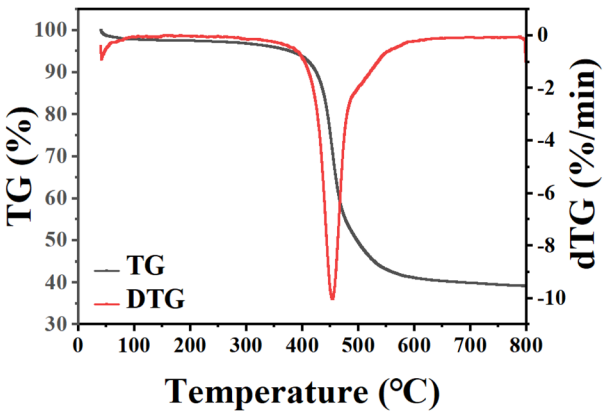

Fig. 1 Thermal stability of NDA-88.

2.2 Adsorption experiments

During the experiment, about 0.5000 g of dried resin was weighed into a quartz glass tube with an inner diameter of 6 mm. High-purity nitrogen and VOCs flowed into the mixing tank, respectively, where the flow rate of all gases was controlled by mass flow controllers to regulate the concentration of VOCs. The mixed gas flows out from the mixing tank and enters the adsorption column with a temperature controlling device for adsorption, and there were sampling ports at the inlet and outlet to test the concentration of VOCs by gas chromatography with an FID detector (GC1100, Beijing China). The diagram of the experimental setup is shown in Fig. 2. The adsorption penetration was considered when the measured VOCs outlet concentration reached 5% of the inlet, and the adsorption equilibrium was considered when the measured VOCs outlet concentration reached 95% of the inlet. The adsorption capacity was calculated using eqn (1) and (2) as follows:

$$Q = Q_1 - Q_2 = C_0 \times V \times t - \int_0^t C \times V \times \mathrm{d}t \quad (1)$$

$$q = \frac{Q}{m} \quad (2)$$

where Q is the dynamic adsorption capacity (mg); Q_1 is the total amount of inlet adsorbed gas (mg); Q_2 is the total amount of outlet adsorbed gas (mg); t is the adsorption time (h); V is the flow volume of carrier gas (160 mL min^{-1}); C is the outlet

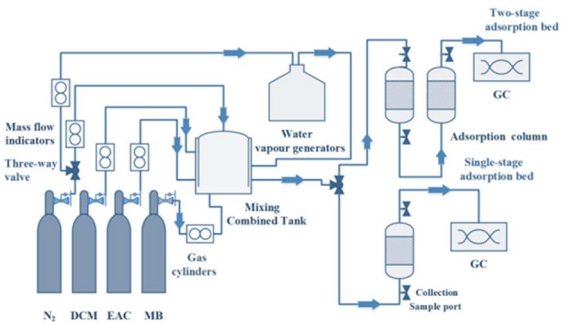

Fig. 2 Flow chart of the experiment.

concentration of the adsorbed gas (mg m^{-3}), and C_0 is the inlet concentration of the adsorbed gas (mg m^{-3}); q is the adsorption capacity per unit mass of adsorbent (mg g^{-1}); m is the adsorbent quality (g). NDA-88 was regenerated by flowing nitrogen gas at a controlled velocity of 160 mL min^{-1} into the adsorption column filled with adsorbed saturated resin at 353 K for more than 2 h until no VOCs were detected in the outlet. The regenerated resin was dried overnight before use.

3 Results and discussion

3.1 Pore characterization of adsorbents

The N_2 adsorption–desorption isotherms at 77 K for NDA-88 are shown in Fig. 3, and the significant properties of the two adsorbents are listed in Table 1. It could be observed that at the initial stage of the adsorption isotherm when the relative partial pressure (P/P_0) is rather low (less than 0.05), the adsorption of nitrogen increased sharply with the increase of the relative pressure, which proves the presence of microporous structures in NDA-88.[17] The sharp increase in nitrogen adsorption is caused by the microporous filling mechanism. As the partial pressure continued to increase, the growth of nitrogen adsorption tended to level off, and when the partial pressure was greater than 0.9, the adsorption amount increased significantly. Significant hysteresis loops were also observed in the N_2 adsorption–desorption isotherms, indicating the presence of mesopores and macropores in the adsorbents. Table 1 shows that NDA-88 has a high specific surface area and microporous and mesoporous structures.

3.2 Equilibrium adsorption of single components

The adsorption isotherms of DCM, EAC, and MB vapors adsorbed by NDA-88 are shown in Fig. 4. The experimental gas velocity is 160 mL min^{-1} with an adsorption temperature of 293 K. The initial concentration of all three gases was 2500 mg m^{-3}. As illustrated in Fig. 4, NDA-88 possessed excellent adsorption capacities for DCM, EAC, and MB, with saturated adsorption quantities of 70.16 mg g^{-1}, 151.06 mg g^{-1}, and 316.46 mg g^{-1}, respectively. As discussed above, a larger specific surface area and pore capacity are favorable for adsorption. The results also demonstrated that the adsorption capacities of NDA-88 for the three gases were in the following order: MB > EAC > DCM. It was because the interaction forces between the three gases and the adsorbent were mainly related to the dispersion forces,[18] which were positively correlated with the molar polarizabilities of the adsorbents, and the molar polarizabilities of the three gases were in accordance with the above order. In addition, the force between the adsorbent and the adsorbate is also associated with the boiling point[19] and the relative molecular mass[17] of the latter; the higher the boiling point and relative molecular mass of the adsorbate, the stronger its force with the absorbent, and the decreasing order of the boiling point and relative molecular mass was MB > EAC > DCM, further confirming the above analysis.

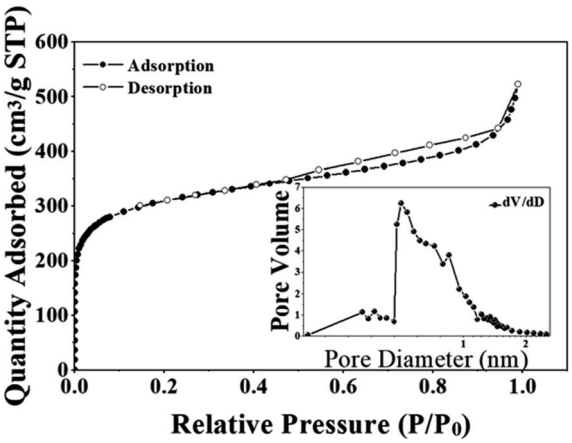

Fig. 3 N_2 adsorption–desorption isotherms of NDA-88 at 77 K.

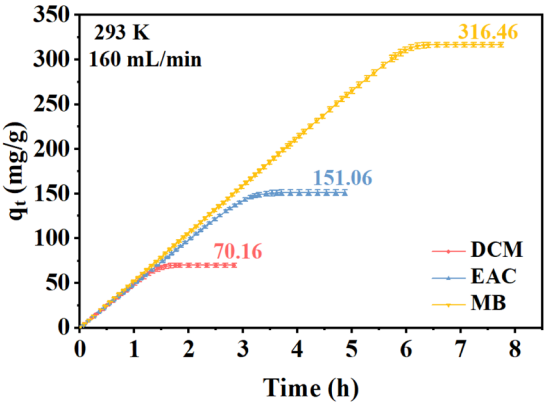

Fig. 4 Breakthrough curves of DCM, EAC, and MB onto NDA-88 in the single vapor system.

3.3 Dynamic adsorption for a binary steam system

In this section, the adsorption capacity of NDA-88 for a mixture of DCM and EAC/MB is investigated. The experiments were conducted at a gas flow rate of 160 mL min^{-1} and 293 K. The inlet concentration of both gases was 2500 mg m^{-3}, and the variation curves of the quantity adsorbed over time are shown in Fig. 5. As shown in Fig. 5, the adsorption of DCM on NDA-88 tended to increase and then decrease in both the binary vapor systems of DCM-EAC and DCM-MB, whereas the adsorption of EAC and MB gradually increased until reaching the maximum. The saturated adsorption of EAC and MB in the binary vapor

Table 1 Structural properties of NDA-88

Adsorbent	S_{BET} (m^2 g^{-1})	S_{micro} (m^2 g^{-1})	V_{meso} (cm^3 g^{-1})	V_{micro} (cm^3 g^{-1})
NDA-88	1240.11	1095.47	0.668	0.479

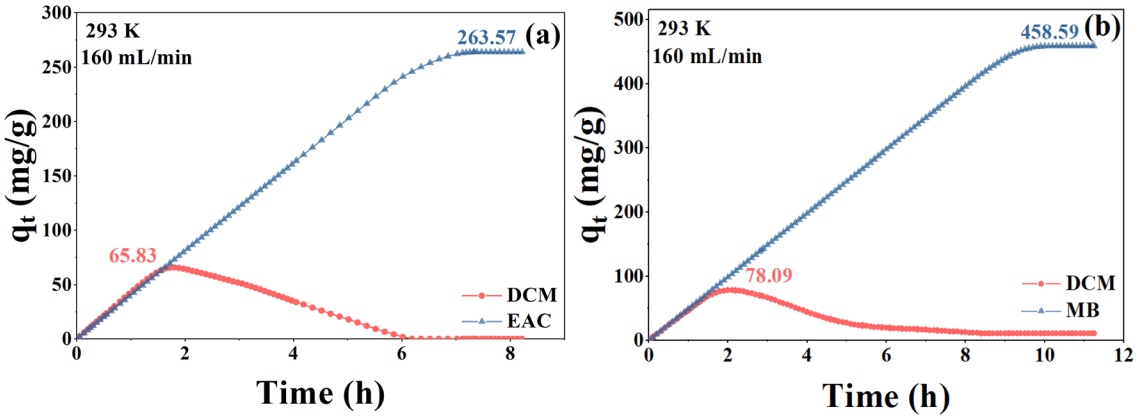

Fig. 5 Plots of adsorbed quantity (q_t) *vs.* time for (a) DCM and EAC, (b) DCM and MB on NDA-88.

system was greater than that of NDA-88 for the single gas above, which improved by 77.5% and 44.9%, respectively.

In the DCM and EAC binary vapor systems, the adsorption of DCM on NDA-88 reached a maximum of 65.83 mg g^{-1}, which is comparable to the saturation capacity of DCM adsorbed onto NDA-88 in the single gas system, and it gradually decreased to 0 when EAC was continuously adsorbed. Therefore, it can be speculated that at the beginning of adsorption, sufficient sites can be provided by NDA-88 for simultaneous adsorption of both DCM and EAC with no obvious competition between them.[20] However, as most of the sites were occupied with the adsorption process, competition between DCM and EAC began to arise. The interaction force between EAC and NDA-88 was stronger than that with DCM, which resulted in the macroscopically adsorbed DCM on NDA-88 being replaced by EAC and flowing out of the matrix together with steam. Remarkably, the presence of DCM promoted the adsorption of EAC by NDA-88 to some extent, probably because the DCM within the resin pores intensified the microporous filling of the EAC.[21] As mentioned before, there were abundant mesopores and micropores in NDA-88, and DCM occupied the resin channel and had no strong interaction with EAC, thus enhancing the adsorption of EAC on NDA-88 by promoting micropore filling of EAC.[22]

In the binary steam systems of DCM and MB, an analogous trend can be observed for the same reason as that mentioned above. In contrast, the maximum adsorption of DCM by NDA-88 in this system reached 78.09 mg g^{-1}, which was slightly higher than the saturation capacity of NDA-88 for a single DCM in the single gas system. As the adsorption of MB was saturated, the adsorption of DCM by NDA-88 was reduced to 10.83 mg g^{-1}. Thus, it can be concluded that the competition between DCM and EAC is stronger than that between DCM and MB.

3.4 Binding power property

This section mainly focuses on the characteristics of the interaction forces between the three gases and NDA-88 in a binary vapor system. The experimental conditions were the same as those in the previous section, with the difference that the two VOCs were not introduced simultaneously, but one gas (*e.g.*, DCM) was introduced first until its penetration and then stopped, at which time the other gas (*e.g.*, EAC or MB) was introduced until its outlet concentration was equal to that of the inlet. The characteristics of the penetration curves of these two components were observed.

As shown in Fig. 6, it can be observed that the adsorption of NDA-88 to all three VOCs is physical because DCM and the other two gases can be substituted for each other. As shown in Fig. 6a, the outlet concentration of EAC suddenly increased and was close to that of the inlet. As shown in Fig. 6c, the outlet concentration of MB gradually increased and was below 2000 mg m^{-3} after the introduction of DCM. Moreover, it can be seen from Fig. S3a and c† that the incoming DCM replaced the adsorbed 15.4% of EAC and 3.2% of MB, respectively, indicating that the interaction force between MB and NDA-88 was stronger than that between EAC and NDA-88 (ref. 23) in the presence of DCM. When comparing Fig. 6b and d, it was observed that the DCM concentration at the outlet increased and later decreased to 0 with the introduction of EAC and MB. Fig. S3b and d† show that the majority of the adsorbed DCM is replaced by EAC/MB, indicating the adsorption force between EAC/MB and NDA-88 was stronger than that between DCM and NDA-88.

In situ FTIR spectra of the adsorption process in each experiment in Fig. 6 were recorded to study the interaction forces (Fig. 7 and S4†). In the DCM and EAC system (Fig. 7), the bands at 2983, 2090, 1748, and 1246 cm^{-1} were assigned to the adsorption of EAC,[24] and the spectra were almost unchanged when DCM was passed in after EAC. When the DCM was passed through first and then the EAC, the absorption peak corresponding to the DCM at 1269 cm^{-1} disappeared gradually.[25] Similar phenomena can be observed in the DCM and MB systems (Fig. S4†), further demonstrating the weak interaction between DCM and NDA-88.

Comparing Fig. 6a–d, it can be found that the penetration time of the second introduced gas in the binary vapor system is shorter than that in the single vapor system after the introduction of another gas, which indicates that DCM competes with the other two gases for adsorption.[26] However, it is known from the previous section that the presence of DCM macroscopically promoted the adsorption of NDA-88 to EAC and MB.

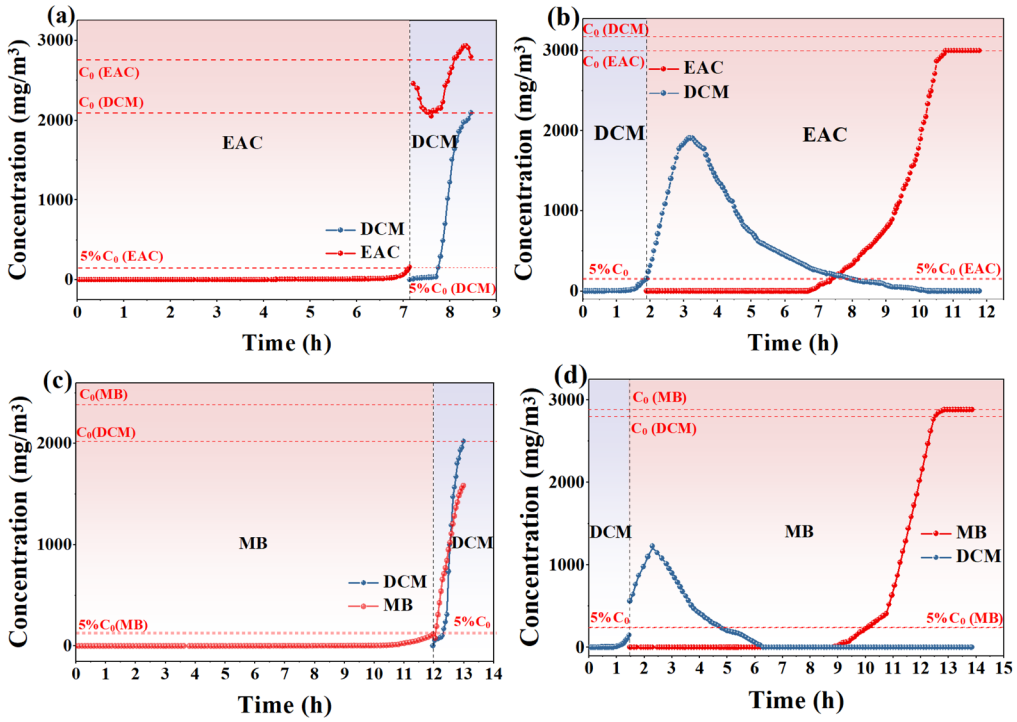

Fig. 6 Adsorption penetration curves under different ventilation conditions on NDA-88. (a) EAC first and then DCM, (b) DCM first and then EAC, (c) MB first and then DCM, (d) DCM first and then MB.

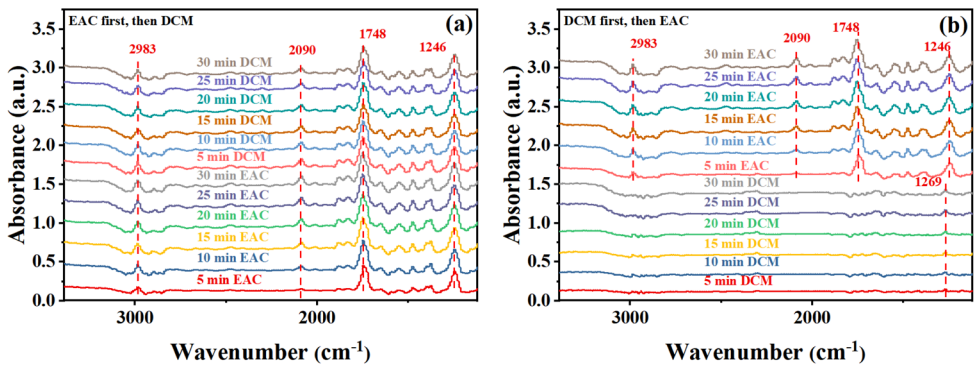

Fig. 7 *In situ* FTIR spectra of (a) EAC followed by DCM, (b) DCM followed by EAC for the adsorption process on NDA-88.

3.5 Co-sorption of DCM with low concentration MB/EAC

This section describes the adsorption characteristics of NDA-88 when DCM was co-adsorbed with low concentrations of MB/EAC. For each experiment, the inlet concentration of DCM was constant at 2500 mg m^{-3} and the concentration of the MB/EAC was adjusted each time. The results are shown in Fig. 8.

According to the results in the above discussions, when NDA-88 adsorbed the same initial concentration of DCM as EAC or MB, the adsorption of DCM was severely hindered because of the competitive adsorption between DCM and EAC or MB. However, Fig. 8a and b show that both low concentrations of EAC and MB could enhance the adsorption of DCM by NDA-88, and their adsorption quantities were larger than the saturation adsorption amount of DCM by NDA-88 (70.16 mg g^{-1}) tested in the single gas system. Specifically, low concentrations of MB enhanced the adsorption of DCM by 28.0–37.6%, whereas low concentrations of EAC boosted the adsorption of DCM by 10.3–35.4%. Moreover, the maximum adsorption of DCM by NDA-88 was achieved when the initial concentration ratio of DCM to MB reached 5.50 : 1, indicating that this concentration ratio was most favorable for the adsorption of DCM with a low concentration of MB in the binary vapor system within the testing scope of this study. Additionally, EAC and MB were not detected at the outlet of the binary vapor system at each initial concentration ratio within the test time (Fig. 8d and e), indicating that NDA-88 has an excellent adsorption capacity for DCM with lower concentrations of EAC or MB systems. As shown in Fig. 8c, the adsorption of NDA-88 for EAC or MB decreased with an

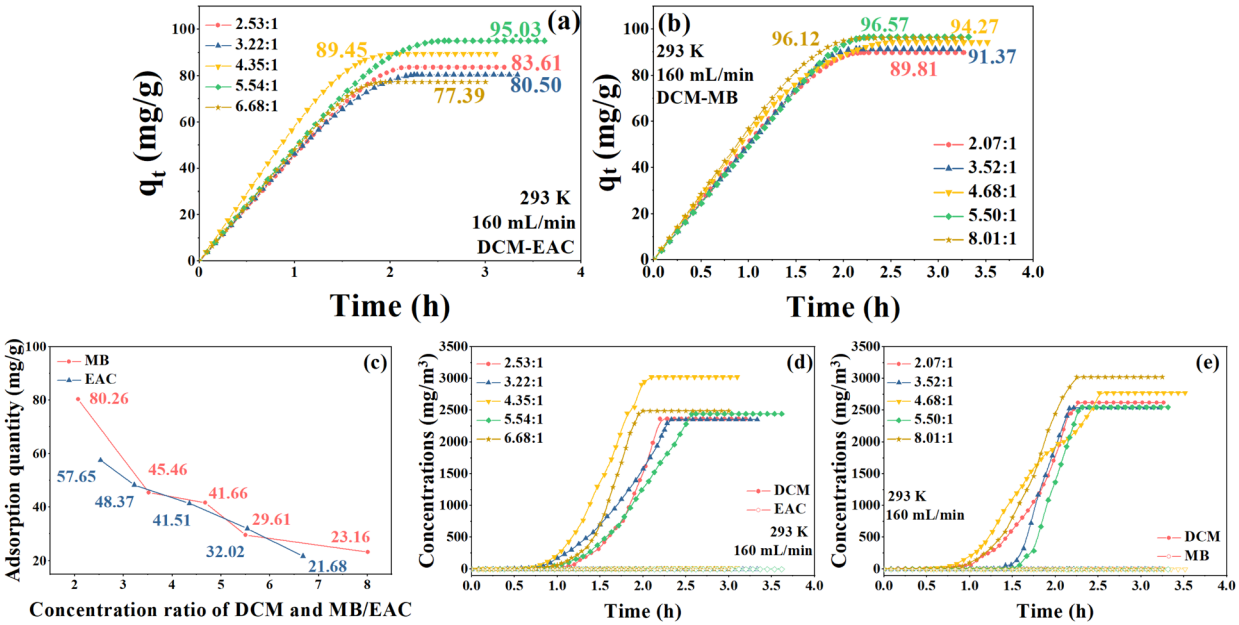

Fig. 8 Plots of the quantity of DCM adsorbed (q_t) *versus* time (t). (a) DCM and EAC system, (b) DCM and MB system, (c) summary of the adsorption quantities of MB and EAC. Plots of the outlet concentration *versus* time. (d) DCM and EAC system, (e) DCM and MB system.

increase in the initial concentration ratio of DCM, which was mainly due to the decrease in the concentration of EAC or MB itself.

Among the experimental groups, on the one hand, the concentrations of EAC and MB were relatively low, and thus NDA-88 had sufficient adsorption sites, and on the other hand, the concentrations of DCM were higher than those of EAC and MB. Therefore, DCM had a more competitive adsorption ability, and the adsorbed DCM was not substituted by EAC or MB.[27] The mechanism of the facilitation effect of low concentrations of EAC or MB on DCM adsorption by NDA-88 was similar to that previously discussed. Specifically, the adsorbed EAC or MB filled the mesopore and macropore voids of NDA-88, which intensified microporous filling of DCM in NDA-88 orifices, thereby increasing the saturation adsorption amount of DCM.

3.6 Effect of water steam on two-component gas adsorption properties

The exhaust gases emitted from the pharmaceutical and chemical industries inevitably contain a certain amount of water, and the moisture content of these gases inevitably fluctuates. When steam is co-adsorbed with a two-component gas containing DCM, competitive adsorption may occur with VOCs. This section investigates the influence of different relative values on the adsorption performance of a mixture of DCM and low concentrations of EAC or MB. The experiments were conducted by controlling the initial DCM concentration to approximately 2500 mg m^{-3}. The specific initial concentration ratios of DCM to EAC or MB and the saturation adsorption capacity of the latter are listed in Table S1.†

The penetration curves of the two-component gases at different relative humidities are shown in Fig. 9a and b. As can be observed from the graphs, the presence of water steam shortens the penetration times of DCM, EAC, and MB in both two-component systems. It was found that water molecules were the first to penetrate when water steam co-adsorbed with VOCs and the penetration rate of water molecules on the same resin with different humidities was almost the same, which was only related to the oxygen-containing functional groups on the resin surface. Water molecules were connected to the functional groups on the surface of NDA-88 through hydrogen bonding and formed water clusters with each other. The water clusters could diffuse into the micropores and mesopores of NDA-88 and compete with VOCs for adsorption sites, leading to a decrease in the adsorption penetration time of the VOCs.

For the saturated adsorption quantities of the samples, as shown in Fig. 9c, in the DCM-EAC binary system, the saturation adsorption of DCM decreased slightly in the relative humidity range of 20–50%, fluctuating from 65.98–70.71 mg g^{-1}. Fig. 9d shows that the adsorption performance of the DCM-MB binary system was strongly influenced by humidity, with the saturation adsorption of DCM dropping from a maximum of 96.12 mg g^{-1} to 54.68 mg g^{-1} under hydrous conditions.

In summary, water steam had a strong influence on the adsorption performance of DCM-MB, leading to a significant decrease in the saturation adsorption capacity of DCM, but still maintained a certain adsorption capacity. While the adsorption performance of the DCM-EAC binary system was less affected by water steam, the penetration time and saturation adsorption capacity of both DCM and EAC decreased.

3.7 Resin regeneration

NDA-88 adsorbed with DCM single-component gas, DCM-MB (concentration ratio of 8.01 : 1), and DCM-EAC (concentration

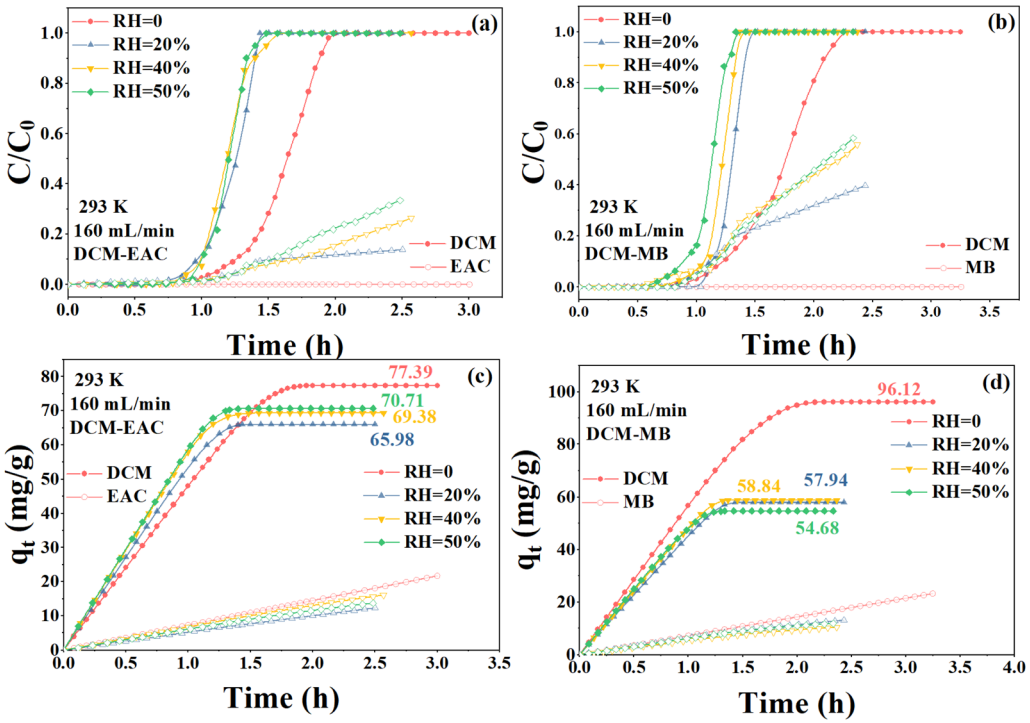

Fig. 9 Sorption penetration curves at different relative humidities (a) DCM-EAC, (b) DCM-MB, sorption volume *versus* time (c) DCM-EAC, (d) DCM-MB.

ratio of 6.68 : 1) binary mixtures were regenerated by hot air regeneration to investigate its recycling performance. The concentration ratios of the components in the binary mixtures are essentially consistent with those in the anhydrous adsorption experiment in Section 3.6. The three sets of resins were subjected to five adsorption and desorption cycles, and the experimental results are shown in Fig. 10.

In the regeneration experiments of DCM single-component adsorption, the saturation adsorption capacity of NDA-88 on DCM after multiple regenerations was greater than that of the first adsorption (70.16 mg g^{-1}), which increased by 26.3–41.8%, showing good regeneration and prolonged recycling performance. The enhanced adsorption capacity of NDA-88 for DCM after regeneration may be due to a change in its pore structure during the regeneration process.

During the regeneration experiments of the DCM-MB binary gas mixture adsorption, the saturation adsorption capacity of NDA-88 for DCM decreased from 11.0% to 13.0% after three regeneration cycles. Namely, its adsorption capacity for DCM did not differ significantly among the three adsorptions. The fifth adsorption cycle showed that the saturation adsorption capacity of DCM further declined slightly (77.44 mg g^{-1}), which was approximately 7.4% lower than that of the fourth adsorption cycle, and the overall adsorption capacity of NDA-88 remained stable. It can be observed from Fig. S6a† that the slopes of the $q_t - t$ curves for the five adsorptions are the same,

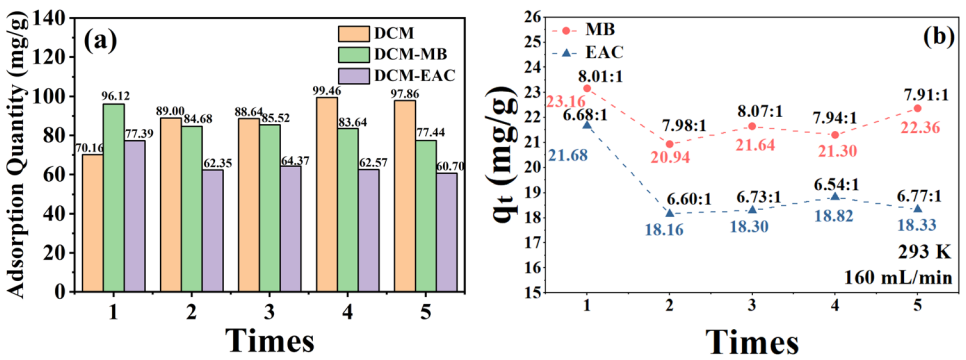

Fig. 10 (a) Plots of dichloromethane adsorption quantity *vs.* time of DCM, DCM-MB, and DCM-EAC system in NDA-88 regeneration experiments, (b) adsorption quantity of MB and EAC by NDA-88 in binary mixture system in each regeneration experiment.

indicating that the adsorption rate of NDA-88 on DCM is almost unchanged.

According to the regeneration experiments of the DCM-EAC binary gas mixture adsorption, the adsorption capacity of NDA-88 for DCM slightly declined after regeneration, and its saturation adsorption capacity was reduced from 16.8% to 21.6%. In contrast to the DCM-MB system, the saturation adsorption capacity of NDA-88 for DCM in the DCM-EAC system at the fifth adsorption was only 2.7% lower than that at the fourth adsorption, and its adsorption capacity was more stable. As observed in Fig. S6b and c,† it can be found that the slope of the $q_t - t$ curves of each group after regeneration is smaller than that of the first adsorption curve, indicating that the adsorption rate of NDA-88 on DCM was slightly reduced after regeneration, but it remained stable after four regenerations.

The amounts of MB and EAC adsorbed in the regeneration experiments with multiple sets of binary gas mixtures are shown in Fig. 10b. As previously described, no MB or EAC was detected at the outlet in each experiment, suggesting that NDA-88 can still completely adsorb MB or EAC in the DCM-low-concentration MB/EAC binary gas mixture within the test time after multiple regenerations. The adsorption amounts of MB and EAC were only dependent on their initial concentrations and the time required for DCM to reach adsorption equilibrium in each experiment. In summary, NDA-88 shows excellent regeneration performance regardless of whether it adsorbs single-component DCM gas or treats a binary mixture of DCM-low-concentration MB/EAC.

4 Conclusions

In this study, DCM, EAC, and MB, the main components of emissions from the pharmaceutical and chemical industries, were used as target pollutants. In view of the complexity of emission components, the large difference in concentration of each component and the water content, a study on the adsorption of each component and mixed exhaust gas containing DCM by hypercrosslinked polymeric resin was carried out.

(1) NDA-88 was excellent for the physical adsorption of DCM, EAC, and MB, with saturated adsorption quantities of 70.16, 151.06, and 316.46 mg g^{-1}, respectively. The magnitudes of the interactions between the three gases and NDA-88 were in the order MB > EAC > DCM.

(2) When NDA-88 adsorbed DCM and MB/EAC at the same inlet concentration, the adsorbed DCM was substituted by MB/EAC because of competitive adsorption. Nevertheless, NDA-88 is suitable for handling binary vapor systems in which DCM is mixed with low concentrations of MB/EAC, and low concentrations of MB/EAC could enhance the adsorption of DCM. This is because the adsorbed MB or EAC intensified the microporous filling of DCM.

(3) The introduction of water steam shortened the penetration times of DCM, EAC, and MB in both the DCM-EAC and DCM-MB two-component systems.

(4) NDA-88 meets the concept of green and sustainable development by achieving good regeneration performance regardless of whether it adsorbs single-component DCM gas or treats DCM-MB/EAC binary gas mixtures.

However, water steam has a relatively significant effect on the properties of NDA-88 for adsorbing two-component gases, and future research could focus on modifying the resin surface groups, particularly reducing the oxygen-containing functional groups,[28] to improve its hydrophobicity.

Conflicts of interest

There are no conflicts to declare.

Acknowledgements

The work was supported by Zhejiang Provincial "Lead Wild goose" Research and Development Project (No. 2022C03073), Science and technology project (2022) of Anqing Future Industrial Technology Research Center of Zhejiang University, Zhejiang Provincial "151" Talents Program, the Program for Zhejiang Leading Team of S&T Innovation (Grant No. 2013TD07).

References

1 V. S. Anithaa, R. Suresh, A. V. Kuklin and S. Vijayakumar, Adsorption of volatile organic compounds on pristine and defected nanographene, *Comput. Theor. Chem.*, 2022, **1211**, 113664.

2 X. Li, L. Zhang, Z. Yang, P. Wang, Y. Yan and J. Ran, Adsorption materials for volatile organic compounds (VOCs) and the key factors for VOCs adsorption process: a review, *Sep. Purif. Technol.*, 2020, **235**, 116213.

3 W. Xiang, X. Zhang, K. Chen, J. Fang, F. He, X. Hu, D. C. W. Tsang, Y. S. Ok and B. Gao, Enhanced adsorption performance and governing mechanisms of ball-milled biochar for the removal of volatile organic compounds (VOCs), *Chem. Eng. J.*, 2020, **385**, 123842.

4 L. P. Guan, Emission characteristics and control ideas of VOCs from industrial source, *Xiandai Huagong*, 2018, **38**, 20–22.

5 Z. Y. Kong, A. Yang, J. G. Segovia-Hernández, A. Putranto and J. Sunarso, Towards sustainable separation and recovery of dichloromethane and methanol azeotropic mixture through process design, control, and intensification, *J. Chem. Technol. Biotechnol.*, 2022, **98**(1), 213–229.

6 R. P. Tong, L. Zhang, X. Y. Yang, J. F. Liu, P. N. Zhou and J. F. Li, Emission characteristics and probabilistic health risk of volatile organic compounds from solvents in wooden furniture manufacturing, *J. Cleaner Prod.*, 2019, **208**, 1096–1108.

7 N. Qiang, T. Z. Shi, T. Liu, Y. Q. Cao, H. C. Miu and J. He, A novel analytical method for the in-depth study of the effects of humidity and temperature on the adsorption of volatile organic compounds, *IOP Conf. Ser.: Earth Environ. Sci.*, 2019, **295**, 012033.

8 X. Yang, H. Yi, X. Tang, S. Zhao, Z. Yang, Y. Ma, T. Feng and X. Cui, Behaviors and kinetics of toluene

adsorption-desorption on activated carbons with varying pore structure, *J. Environ. Sci.*, 2018, **67**, 104–114.

9 S. Jafari, F. Ghorbani-Shahna, A. Bahrami and H. Kazemian, Adsorptive removal of toluene and carbon tetrachloride from gas phase using zeolitic imidazolate framework-8: effects of synthesis method, particle size, and pretreatment of the adsorbent, *Microporous Mesoporous Mater.*, 2018, **268**, 58–68.

10 M. Jahandar Lashaki, J. D. Atkinson, Z. Hashisho, J. H. Phillips, J. E. Anderson and M. Nichols, The role of beaded activated carbon's pore size distribution on heel formation during cyclic adsorption/desorption of organic vapors, *J. Hazard. Mater.*, 2016, **315**, 42–51.

11 Y. Wang, X. Su, Z. Xu, K. Wen, P. Zhang, J. Zhu and H. He, Preparation of surface-functionalized porous clay heterostructures via carbonization of soft-template and their adsorption performance for toluene, *Appl. Surf. Sci.*, 2016, **363**, 113–121.

12 X. Li, L. Zhang, Z. Yang, P. Wang, Y. Yan and J. Ran, Adsorption materials for volatile organic compounds (VOCs) and the key factors for VOCs adsorption process: a review, *Sep. Purif. Technol.*, 2020, **235**, 116213.

13 B. Zhou, B. Sun, W. Qiu, Y. Zhou, J. He, X. a. Lu and H. Lu, Adsorption/desorption of toluene on a hypercrosslinked polymeric resin in a highly humid gas stream, *Chin. J. Chem. Eng.*, 2019, **27**(4), 863–868.

14 H. Liu, Y. Yu, Q. Shao, C. J. S. Long and P. Technology, Porous polymeric resin for adsorbing low concentration of VOCs: Unveiling adsorption mechanism and effect of VOCs' molecular properties, *Sep. Purif. Technol.*, 2019, **228**, 115755.

15 X. Xia, P. Sun, X. Sun, Y. Wang, S. Yang, Y. Jia, B. Peng and C. Nie, Hyper-crosslinked polymers with controlled multiscale porosity for effective removal of benzene from cigarette smoke, *ePolymers*, 2022, **22**, 19–29.

16 J. Wang, W.-Q. Wang, Z. Hao, G. Wang, Y. Li, J. Chen, M. Li, J. Cheng and Z.-T. Liu, A superhydrophobic hyper-crosslinked polymer synthesized at room temperature used as an efficient adsorbent for volatile organic compounds, *RSC Adv.*, 2016, **6**, 97048–97054.

17 H. Liu, Y. Yu, Q. Shao and C. Long, Porous polymeric resin for adsorbing low concentration of VOCs: unveiling adsorption mechanism and effect of VOCs' molecular properties, *Sep. Purif. Technol.*, 2019, **228**, 115755.

18 J. Mahanty and B. W. Ninham, Dispersion forces in physical adsorption, *J. Chem. Soc., Faraday Trans. 2*, 1974, **70**, 637–650.

19 C. Long, Q. Li, Y. Li, Y. Liu, A. Li and Q. Zhang, Adsorption characteristics of benzene–chlorobenzene vapor on hypercrosslinked polystyrene adsorbent and a pilot-scale application study, *Chem. Eng. J.*, 2010, **160**(2), 723–728.

20 K. Ramanathan, C. K. Koch and S. H. Oh, Kinetic modeling of hydrocarbon adsorbers for gasoline and ethanol fuels, *Chem. Eng. J.*, 2012, **207–208**, 175–194.

21 A. E. Grinchenko, E. E. Men'shchikova, I. E. Men'shchikov, A. V. Shkolina and A. A. Fomkin, Estimation of adsorption of ethane on the superactive microporous carbon adsorbent using the theory of volume filling of micropores, *Russ. Chem. Bull.*, 2020, **69**(11), 2091–2096.

22 C. Balzer, R. T. Cimino, G. Y. Gor, A. V. Neimark and G. Reichenauer, Deformation of Microporous Carbons during N_2, Ar, and CO_2 Adsorption: Insight from the Density Functional Theory, *Langmuir*, 2016, **32 32**, 8265–8274.

23 G. Wang, B. Dou, Z. Zhang, J. Wang, H. Liu and Z. Hao, Adsorption of benzene, cyclohexane and hexane on ordered mesoporous carbon, *J. Environ. Sci.*, 2015, **30**, 65–73.

24 Y. Cai, X. Zhu, W. Hu, C. Zheng, Y. Yang, M. Chen and X. Gao, Plasma-catalytic decomposition of ethyl acetate over $LaMO_3$ (M = Mn, Fe, and Co) perovskite catalysts, *J. Ind. Eng. Chem.*, 2019, **70**, 447–452.

25 S. Cao, H. Wang, F. Yu, M. Shi, S. Chen, X. Weng, Y. Liu and Z. Wu, Catalyst performance and mechanism of catalytic combustion of dichloromethane (CH_2Cl_2) over Ce doped TiO_2, *J. Colloid Interface Sci.*, 2016, **463**, 233–241.

26 M. Ouzzine, A. J. Romero-Anaya, M. A. Lillo-Ródenas and A. Linares-Solano, Spherical activated carbons for the adsorption of a real multicomponent VOC mixture, *Carbon*, 2019, **148**, 214–223.

27 C. Long, W. Yu and A. Li, Adsorption of n-hexane vapor by macroporous and hypercrosslinked polymeric resins: equilibrium and breakthrough analysis, *Chem. Eng. J.*, 2013, **221**, 105–110.

28 L. Jia, B. Niu, X. Jing, Y. Wu and W. M. Association, Equilibrium and hysteresis formation of water vapor adsorption on microporous adsorbents: effect of adsorbent properties and temperature, *J. Air Waste Manage. Assoc.*, 2021, **72**, 176–186.